Cell. Mol. Life Sci. 63 (2006) 367–377
1420-682X/06/030367-11
DOI 10.1007/s00018-005-5510-8

Cellular and Molecular Life Sciences

Research Article

Disruption of clc-5 leads to a redistribution of annexin A2 and promotes calcium crystal agglomeration in collecting duct epithelial cells

G. Carr[a], N. L. Simmons[a] and J. A. Sayer[a, b]

[a] Institute for Cell and Molecular Biosciences, Medical School, University of Newcastle upon Tyne, NE2 4HH (United Kingdom), Fax: +44 191 222 6706, e-mail: j.a.sayer@ncl.ac.uk
[b] School of Clinical Medical Sciences, Medical School, University of Newcastle upon Tyne, NE2 4HH (United Kingdom)

Received 22 October 2005; received after revision 26 November 2005; accepted 2 December 2005
Online First 25 January 2006

Abstract. Mutations in *CLCN5,* which encodes the voltage-dependent Cl^-/H^+antiporter, CLC-5, cause Dent's disease. This disorder is characterized by low molecular-weight proteinuria, hypercalciuria, nephrocalcinosis and nephrolithiasis. Using a collecting duct cell model (mIMCD-3) in which endogenous clc-5 is disrupted by antisense *clc-5* or overexpression of truncated *clc-5*, we demonstrate altered expression of the crystal adhesion molecule, annexin A2. Endogenously expressed annexin A2 is intracellular with limited plasma membrane localization. Following clc-5 disruption, there is both a marked increase in plasma membrane annexin A2 and an increase in cell surface crystal retention and agglomeration, which may be attenuated using pretreatment with anti-annexin A2 antibodies or wheat germ agglutinin lectin but not by concanavalin A. We hypothesize that in Dent's disease, endocytic failure leads to an accumulation at the plasma membrane of crystal-binding molecules that include annexin A2 leading to retention of calcium crystals and ultimately nephrocalcinosis and nephrolithiasis.

Key words. Collecting duct; Dent's disease; kidney stones; renal epithelial cell; endocytosis; nephrocalcinosis.

CLC-5 is a voltage-gated chloride channel/voltage-dependent Cl^-/H^+ antiporter [1, 2] expressed in the proximal tubule, thick ascending limb of Henle and the collecting duct of the human kidney [3–5]. Mutations in *CLCN5,* which encodes CLC-5, underlie the X-linked disorder, Dent's disease [3]. Affected males have a renal phenotype that includes low molecular-weight proteinuria, hypercalciuria and hyperphosphaturia [3, 6]. Although a loss of CLC-5 has been shown to result in defective endocytosis within the proximal tubule [7–9] and *clc-5* knockout mice invariably display proteinuria and commonly hypercalciuria/hyperphosphaturia [8, 10, 11], the pathophysiological progression to nephrocalcinosis and renal stones remains uncertain.

Stone formation requires formation of crystals followed by their retention and accumulation in the kidney. Crystal retention and accumulation are critically dependent upon the interaction between the renal tubular epithelial surfaces and urinary microcrystals, which may attach to the epithelial surface and form a nucleus for further crystal agglomeration and stone formation [12]. Such interactions are most likely to occur at the point of maximal tubular solute concentration (e.g. the medullary collecting duct) [13]. In a murine inner medullary collecting duct cell model (mIMCD-3), we have previously reported disruption of endogenous clc-5 protein expression by using an antisense approach. Transfection of mIMCD-3

* Corresponding author.

cells with a full-length antisense *clc-5* transcript reduces clc-5 protein expression, which leads to a failure to acidify recycling endosomes and an arrest of endocytosis [14, 15]. Importantly, clc-5 disruption also leads to increased attachment and agglomeration of both calcium oxalate and calcium phosphate crystals onto the cell surface in mIMCD-3 cells [15]. In this instance, the cell surface properties or the presence of a functional crystal 'receptor' must have been altered.

Recently, Kumar et al. [16] identified annexin A2 (alias annexin II) as a crystal-binding molecule in renal epithelial (MDCK1) cells. Annexin A2 belongs to the multigene annexin protein family, implicated in numerous cellular and membrane functions including membrane trafficking, exocytosis/endocytosis, membrane-cytoskeleton interactions, ion transport and cell-cell adhesion [17–21]. Annexins often reside in both a cytosolic and a membrane-associated pool, with a switch between the two typically being regulated by calcium [22]. Within the cell, membrane-bound annexin A2 is found at the plasma membrane and on membranes of the biosynthetic or endocytic pathway [22, 23]. Due to this location, its ability to aggregate membrane vesicles and the fact that it colocalizes with caveolin I [16], annexin A2 has been implicated in membrane traffic, both in the regulated exocytic pathway [24] and the endocytic pathway [25, 26]. Annexin A2 is localized on the external membrane of some cells where it can function as a receptor for lipid A [27], cytomegalovirus [28], vitamin $1,25(OH)_2D_3$ [29], β2-glycoprotein I [30], t-PA, plasminogen [31] and tenascin-C [32]. In MDCK cells, extracellular anti-annexin A2 antibodies prevented calcium oxalate monohydrate (COM) crystal adhesion, suggesting that annexin A2 is present on the exofacial surface of the apical plasma membrane [16]. A number of other membrane surface molecules may be associated with increased crystal adhesion to apical renal surfaces. Wheat germ agglutinin (WGA) lectin has affinity for sialic acid-containing glycoproteins and has been shown to decrease adhesion of calcium oxalate or phosphate crystals [12, 33]. Studies with renal tubular cells in culture and with ethylene glycol-induced renal tubular cell damage in rats have shown that hyaluronan, osteopontin and their mutual cell surface receptor, CD44, also play an important role in calcium oxalate crystal binding [34, 35]. Such molecules are not present at the apical surface in normal tubular epithelium but appear after cell damage during wound healing/regeneration [34, 35].

Since clc-5 disruption appears to predispose the renal epithelium to crystal adhesion/retention, the primary aim of this study was to investigate the effect of clc-5 disruption upon the candidate crystal adherence molecule, annexin A2, in the mIMCD-3 cell model. A secondary question was whether annexin A2 dysregulation occurs in association with other surface proteins. By using transfection with antisense *clc-5* cDNA to disrupt endogenous clc-5 and by overexpression of truncating mutants of *clc-5*, we demonstrate that the resultant increase in crystal binding was prevented by anti-annexin A2 antibodies and WGA lectin, implicating both annexin A2 plasma membrane overexpression and sialic acid residues in the pathophysiology of Dent's disease.

Materials and methods

Molecular reagents. mIMCD-3 cells were cultured as previously described [36]. mIMCD-3 total RNA was isolated (Qiagen) and used as the template for RT-PCR reactions using mouse gene specific primer pairs for *annexin A2* transcript 2 (5′-TTC AAA ATG TCT ACT GTC CAC GAA ATC-3′ and 5′-TGA GCC CTT CAG TCA TCC CCA-3′). *annexin A2* was cloned into expression vector pcDNA3.1/NT-*GFP* (Invitrogen Life Technologies) and directly sequenced to confirm orientation and fidelity of the *annexin-A2-GFP* fusion protein construct. Murine *clc-5* plasmid DNA constructs included wild-type *clc-5* (sense), *clc-5* with an N-terminal green fluorescent protein (*GFP*) fusion (*clc-5-GFP*), antisense *clc-5* (AS-*clc-5*) and three N-terminal *GFP*-tagged *clc-5* constructs with truncating mutations (R648X, R695delCfs or R704X) termed mutant *clc-5*, as previously described [14, 37].

Cellular localization of annexin A2. mIMCD-3 cells were grown to near confluency on 13 mm coverslips. Cells were fixed and permeabilized with methanol. Annexin A2 was detected, after incubation in horse serum, by a rabbit anti-annexin A2 polyclonal antibody (H-50 raised against residues 1–50 of the human protein but cross-reactive with mouse) at 1:50 (Santa Cruz Biotechnology), followed by a secondary block with goat serum and then goat anti-rabbit TRITC (1:100 and 1:25, respectively, Sigma) for secondary detection. Control experiments omitted the primary antibody or used preimmune rabbit serum instead of primary antibody (both negative). Alternatively, mIMCD-3 cells were transiently transfected with *annexin A2-GFP* using the Lipofectamine 2000 reagent (Life Technologies) following the manufacturer's protocol. Twenty-four hours after transfection, live cells were incubated with TRITC-WGA lectin (1:50, Sigma) for 2 min at 37 °C to label the plasma membrane, or 75 nM LysoTracker Red (Molecular Probes) for 30 min at 37 °C to label acidic endosomes. Cotransfection with pDsRED-ER (BD Biosciences) allowed identification of endoplasmic reticulum (ER). For staining of the Golgi apparatus (intermediate-to-*trans* stacks), cells were fixed and permeabilised 24 h post-transfection with methanol then incubated (room temperature) with biotinylated *Griffonia* lectin (20 µg/ml; Vector Laboratories) for 30 min, followed by streptavidin-Cy5 (20 µg/ml; Southern Biotech) for 1 h at 37 °C.

Annexin A2 distribution and endocytosis following transfection. mIMCD-3 cells were first transiently transfected with AS-*clc-5* together with pcDNA3.1/*GFP* (*GFP*) as a transfection marker (microgram ratio of 3:1). Control cells were transfected with *GFP* alone. In separate experiments, mIMCD-3 cells were transfected with *clc-5-GFP* or mutant *clc-5-GFP* cDNA. Twenty-four hours after transfection, cells were fixed and permeabilized with methanol. Annexin A2 was detected using the anti-annexin A2 antibody as described previously.
In separate experiments, 24 h following *clc-5-GFP* or mutant *clc-5-GFP* construct transfection, WGA lectin internalization by endocytosis after 1 h lectin incubation was quantified using mid-cell *xy* sections of positive transfectants and compared directly to neighbouring cells. Qwin software (Leica UK) was used to express lectin-positive pixels as a percentage of total cell area.

Microscopy. Cells were imaged using confocal laser scanning microscopy (TCS-NT, Leica with Kr-Ar laser) using appropriate excitation and emission filter sets for dual fluorophore detection, and *z*-series images were collected. Mid-cell (*xy*) sections of cells transfected with *annexin-A2-GFP* (costained with TRITC-WGA), AS-*clc-5* or mutant *clc-5-GFP* together with appropriate controls (empty-vector *GFP* or *clc-5-GFP* as indicated) were used to quantify annexin A2 protein expression by analysis of pixel intensity. For 'membrane' localization, four circumferential transects per cell were drawn progressing clockwise around the cell under identical conditions of imaging, illumination intensity and photo-multiplier settings. Pixel intensity was then determined from background (near membrane but extracellular) values to the adjacent (often peak) pixel at the cell periphery. This averaged intensity (eight readings per cell) was then defined as membrane (peripheral) annexin A2 staining.

COM adhesion/agglomeration to cells pretreated with anti-annexin A2 antibody or lectin. COM crystal adhesion/agglomeration was performed by incubation (after a brief wash in PBS) with preformed COM crystals, as previously described [15], for 30 min at 37 °C. Cells were washed again in PBS (to remove any non-attached crystals) and then imaged by confocal microscopy as described before. For each positive transfectant, the cell surface attachment of COM crystals was analyzed by a simple scoring method of no crystal attachment, crystals of ≤10 μm attached and crystal agglomerations >10 μm in randomly selected transfectants (×100 lens, NA 1.4). The effect of expression of truncating mutations (R648X, R695delCfs or R704X) with wild type *clc-5-GFP* was tested 24 h posttransfection on crystal adhesion/agglomeration as above.
To test for a direct role of annexin A2 in COM crystal agglomeration, mIMCD-3 cells were transfected with *GFP* (control) or antisense *clc-5* and *GFP* as a transfection marker (microgram ratio of 3:1), blinded to treatment type. Twenty-four hours after transfection, cells were washed in PBS and then incubated with 200 μl blocking solution or anti-annexin A2 antibody (4 μg/ml) in blocking solution at room temperature for 15 min.
The role of sialic acid residues was tested by preincubation of transfected cells [control (*GFP*), sense *clc-5* and *GFP* as a transfection marker or AS-*clc-5* and *GFP*] with TRITC-WGA lectin (100 μg/ml in PBS, 2 min at 37 °C; Vector Laboratories), prior to washing in PBS and exposure to COM crystals as described before. Controls for WGA treatment included TRITC-concanavalin A (α-mannapyranosyl/α-glucopyranosyl specific) pretreatment (100 μg/ml in PBS, 2 min at 37 °C; Vector Laboratories) or culture medium alone without lectin.

Statistics. Plasma membrane pixel intensity (arbitrary units) of annexin A2 and lectin internalization was compared using Student's t-test. Crystal attachment and agglomeration were compared in respective treatment groups by Chi-square analysis or Student's t-test.

Results

Annexin A2 expression and localization in mIMCD-3 cells. mIMCD-3 cells endogenously express annexin A2 as detected by RT-PCR (fig. 1A). Immunolocalization of annexin A2 (fig. 1B) revealed a diffuse intracellular distribution with limited localization at the plasma membrane.
To more precisely determine the subcellular localization of annexin A2, mIMCD-3 cells were transfected with *annexin A2-GFP* and colocalized with plasma membrane and intracellular organelle markers (fig. 1C–H). Cells counter-stained with extracellular TRITC-WGA lectin revealed a punctate cytoplasmic distribution with a subset of annexin A2 present at the plasma membrane as demonstrated by colocalization with WGA lectin (fig. 1C, D) and a transect depicting pixel intensity across the section (fig. 1E). Note that TRITC-WGA (red) gives a sharp increase in pixel intensity from background levels as the membrane is crossed corresponding to a peak of *annexin A2-GFP* intensity (green, fig. 1E). Additional assessment of the subcellular distribution of annexin A2 was obtained using subcellular markers. *Griffonia* lectin (as a marker of the intermediate-to-*trans* stacks of the Golgi apparatus) colocalized in part with annexin A2-*GFP* (fig. 1F). The marker pDsRED2-ER, which utilizes calreticulin/KDEL to target the fusion protein to the ER, also showed extensive colocalization with annexin A2-*GFP* (fig. 1G). LysoTracker Red is an acidic endosomal marker, which we have previously shown to colocalize with clc-5 in mIMCD-3 cells [36]. *Annexin A2-GFP*

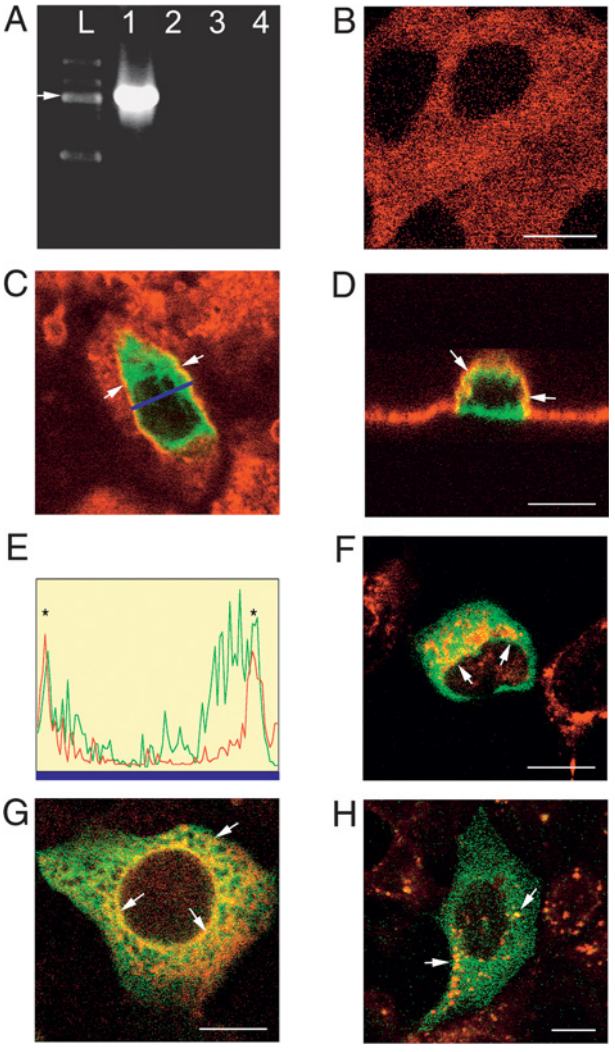

Figure 1. Annexin A2 expression and localization in mIMCD-3 cells. (*A*) *annexin A2* (transcript 2, 1 kb, arrowed) was amplified using high-fidelity RT-PCR from mIMCD-3 cell RNA (lane 1). RT controls omitted either RNA (lane 2) or reverse transcriptase enzyme (lane 3) and a PCR control used water as template (lane 4). L, 100 bp DNA ladder Plus. (*B*) Immunolocalization of annexin A2 (red) in mIMCD-3 cells. Note the diffuse nature of cytoplasmic staining. (C–E) Cells transfected with *annexin A2-GFP* (green) and costained with TRITC-WGA (used as a plasma membrane marker) demonstrate a degree of colocalization at the cell periphery (yellow, arrowed) in both *xy* (*C*) and *xz* (*D*) sections. Quantification of pixel intensity (arbitrary units) for a mid-cell transect (blue bar shown in *C*) depicts *annexin A2-GFP* (green) and lectin (red) with colocalization of markers marked with an asterix (*E*). Colocalization (yellow, arrowed) of *annexin A2-GFP* (green) and subcellular markers (red) is demonstrated with the Golgi-staining *Griffonia* lectin (*F*), ER marker pDsRED2-ER (*G*) and acidic endosomal marker LysoTracker Red (*H*). Scale bar, 10 µm.

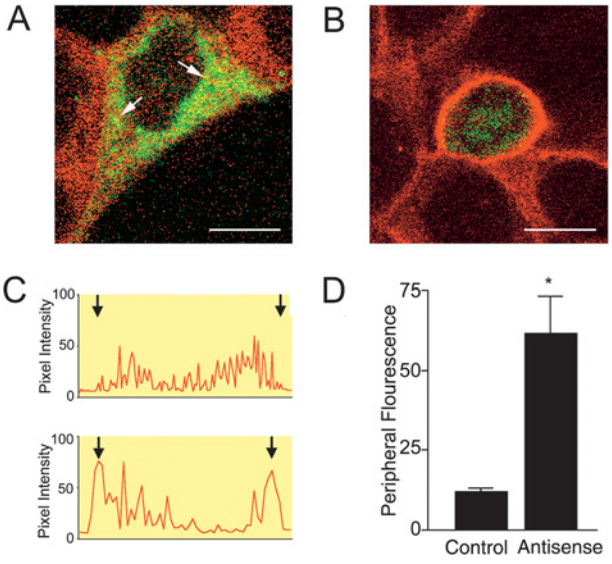

Figure 2. Antisense *clc-5* transfection leads to a redistribution of annexin A2 in mIMCD-3 cells. (*A*) Transfection of mIMCD-3 cells with sense *clc-5-GFP* (green) shows unaltered cytosolic/periplasma membrane distribution of annexin A2 (as detected by annexin A2 antibody staining). A minor degree of colocalization (yellow areas, arrowed) is observed. (*B*) An antisense *clc-5* transfectant (cotransfected with *GFP*) shows markedly increased annexin A2 immunostaining (red) at the cell periphery compared to surrounding non-transfected cells and *clc-5-GFP*-transfected cells (shown in *A*). Scale bar, 10 µm (*C*) Sample cell transects depicting pixel intensity of annexin A2 antibody for control cell (top transect) and *clc-5*-disrupted cells (bottom transect). Arrows show the outermost peaks used in the measurement of peripheral annexin A2. (*D*) Quantification of annexin A2 immunofluorescence at the cell periphery in control *GFP*- and antisense *clc-5*/*GFP*-transfected cells. Pixel intensity (arbitrary units) of anti-annexin A2 antibodies is shown (detected using anti-rabbit TRITC at a 1:25 dilution). Annexin A2 immunostaining was increased in antisense *clc-5*-transfected cells compared to controls (61.46 ± 11.79, n = 6 compared to 11.88 ± 1.44, n = 3, *p < 0.05).

demonstrates only a minor degree of colocalization with LysoTracker Red (fig. 1H).

Annexin A2 redistribution following clc-5 manipulation. mIMCD-3 cells were transiently transfected with *clc-5-GFP* then fixed and stained with anti-annexin A2 antibody. This revealed that the extensive endosomal distribution of *clc-5* remained distinct from that of annexin A2 (fig. 2A) with only minor areas of colocalization, as expected from the degree of colocalization of annexin A2 with LysoTracker Red (fig. 1H). It should also be noted that the distribution of annexin A2 was unaffected by overexpression of *clc-5-GFP* (fig. 2A) or by transfection of *GFP* alone (image not shown). In contrast, following transfection of AS-*clc-5* (together with *GFP* as transfection marker), there was a marked redistribution of cytoplasmic annexin A2 to the cell periphery (fig. 2B). Mid-cell *z*-section transects (sample transects depicted in fig. 2C) were analyzed, and quantification of annexin A2 antibody staining at the cell margin was performed using two secondary (fluorescent) antibody dilutions, 1:100 and 1:25, respectively. Cell periphery pixel intensity (arbitrary units) of annexin A2 increased from 13.20 ± 1.17 (n = 7) in control (*GFP*-transfected) cells to 30.49 ± 2.53

($n = 15$, $p < 0.0005$) after AS-*clc-5* transfection, in the 1:100 group. Similarly, cell periphery pixel intensity for annexin A2 was significantly increased in AS-*clc-5*-transfected cells (61.46 ± 11.79) compared to control cells (11.88 ± 1.44, $p < 0.05$) using a 1:25 dilution of secondary antibody (fig. 2D).

Calcium crystal agglomeration promoted by antisense *clc-5* treatment may be blocked with anti-annexin A2 antibodies. Qualitatively, when AS-*clc-5*-transfected cells were overlaid with preformed COM crystals there was retention and agglomeration compared to *GFP*-transfected cells (fig. 3A, C), in confirmation of our previously published data [14, 15]. Native cells had only a limited capacity to bind COM crystals. In antisense *clc-5*-transfected cells, a marked quantitative difference in crystal agglomeration (17/30 cells) was evident in comparison to control *GFP*-transfected cells (3/33, $p < 0.005$, fig. 3E). To investigate whether the antisense *clc-5*-promoted crystal agglomeration was mediated directly by the redistribution of the crystal adhesion molecule, annexin A2, to the plasma membrane, the effect of extracellular treatment with anti-annexin A2 antibody prior to exposure to calcium crystals was tested. Control data included preincubation with blocking serum as compared to anti-annexin A2 (in blocking serum). In cells treated with anti-annexin A2 prior to exposure to calcium oxalate crystals there was a clear protective effect against crystal agglomeration despite AS-*clc-5* transfection (fig. 3D, F). In the anti-annexin antibody-treated groups, there was no significant difference between numbers of crystal agglomerations (2/21 antisense, and 2/34 control *GFP*, ns, fig. 3B, D, F). Comparing the number of crystal agglomerations in antisense *clc-5* transfectants alone, anti-annexin A2 reduced the number of cells with crystal agglomerations from 57% to just 10% ($p < 0.005$, fig. 3E, F).

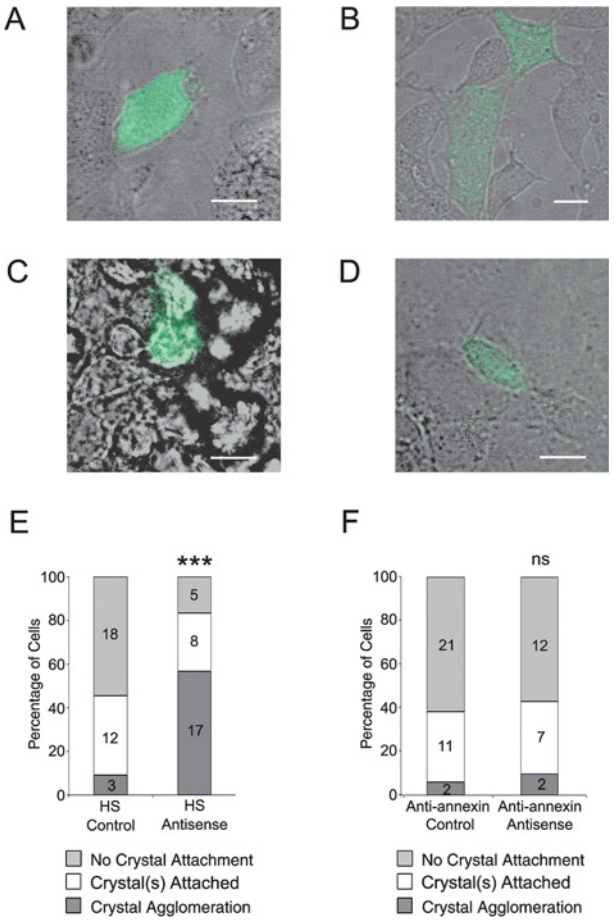

Figure 3. Antisense *clc-5* transfection promotes calcium oxalate crystal agglomeration which is blocked by pre-exposure to anti-annexin A2 antibody. (*A–D*) Comparison of mIMCD-3 cells transiently transfected 24 h prior to exposure to calcium oxalate crystals with control *GFP* alone (*A, B*), or cotransfected with antisense *clc-5* and *GFP* (*C, D*), then preincubated with blocking solution (*A*, *C*) or anti-annexin A2 antibody (*B*, *D*). Positive transfectants are identified by their green fluorescence. Note agglomerated crystals are above the focal plane of the apical surface of the transfected cells (*C*). Scale bar, 10 µm. (*E*, *F*) Quantification of calcium oxalate crystal attachment to control *GFP*- and antisense *clc-5*/*GFP*-cotransfected cells. (*E*) Transfectants treated with blocking solution before crystal exposure: agglomerations were seen in 3/33 control *GFP* cells compared to 17/30 of antisense *clc-5* transfectants (***$p < 0.005$). (*F*) Transfectants treated with anti-annexin A2 antibody before crystal exposure: crystal agglomeration was limited in antisense *clc-5*-treated cells and did not differ from *GFP* controls.

Overexpression of mutant *clc-5* in mIMCD-3 cells is associated with a disruption in endocytosis, annexin A2 redistribution and COM crystal agglomeration. Previously, we have shown that certain truncating mutations of *clc-5* disrupt CBS domain 2 of CLC-5 and give rise to a trafficking defect [37]. Since CLC-5 is a dimeric protein [37, 38], we hypothesized that overexpression of CLC-5 mutant proteins may disrupt traffic of endogenous CLC-5 and produce a similar phenotype to that seen for AS-*clc-5*-transfected cells. We have also previously demonstrated that following antisense *clc-5* transfection, a dramatic disruption in endocytosis of WGA lectin in mIMCD-3 cells is observed [14]. Transfection of cDNA encoding truncated forms of clc-5, which disrupt the C-terminal CBS domain 2, also produced a similar interruption of endocytosis (fig. 4). Cells transfected with either *clc-5-GFP* (wild-type) or mutant *clc-5-GFP* were compared to neighbouring non-transfected cells, following incubation with WGA lectin. WGA lectin was readily endocytosed to an intracellular location in non-transfected and *clc-5-GFP* transfected cells. In contrast, with overexpression of truncated forms of *clc-5*, which correspond to three *CLCN5* mutations R648X, 695delCfs, and R704X, the WGA lectin remained localized near the plasma membrane location, with limited internalization after 1 h (fig. 4).

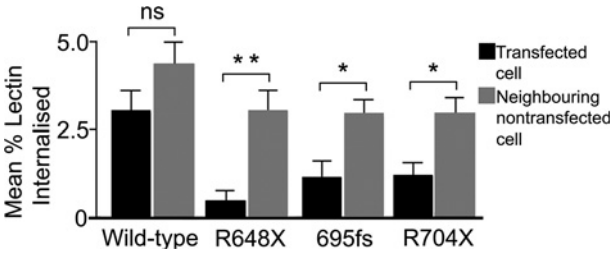

Figure 4. Overexpression of truncated *clc-5* causes an arrest of lectin internalization in mIMCD-3 cells. Internalization of TRITC-WGA was compared in mIMCD-3 cells transiently transfected with wild-type or mutant *clc-5* following 1 h incubation. Transfectants were compared to neigbouring non-transfected cells. There was no significant difference in lectin internalization between wild-type transfectants (n = 11) and their neighbouring non-transfected cells (n = 13). Following overexpression of three mutant *clc-5* cDNA constructs (R648X, n = 10; 695delCfs, n = 16; R704X, n = 16), lectin internalization was significantly reduced when compared to neighbouring non-transfected cells (n = 13, $p < 0.005$; n = 20, $p < 0.05$; n = 22, $p < 0.05$, respectively).

Corresponding to this failure of endocytosis, transfection of mIMCD-3 cells with the *clc-5* mutants R648X, 695delCfs and R704X (fig. 5A, B and C, respectively), all markedly increased the peripheral (plasma membrane) localization of annexin A2 in a similar manner to that seen for antisense *clc-5* transfection (described earlier). Peripheral 'membrane' intensity (see Materials and methods) of anti-annexin A2 (using secondary antibody 1:25) in the mutant *clc-5-GFP*-transfected cells was 51.14 ± 5.34 (n = 13) compared to 24.22 ± 2.13 (n = 8) in *clc-5-GFP*-transfected cells ($p < 0.005$) (fig. 5D). Overexpression of mutant *clc-5* proteins thus gave rise to a similar phenotype to antisense *clc-5* transfection, with a marked redistribution of annexin A2 from an intracellular location to an apparent plasma membrane localization.

Using the GFP-tagged R704X *clc-5* mutant, we analyzed the response of transfected cells to COM crystal overlay comparing them to wild-type *clc-5-GFP*-transfected cells (fig. 5E, F). Quantification of crystal attachment and agglomeration showed that whereas the majority of cells transfected with *clc-5-GFP* showed no crystal attachment or attachment of crystals of small size (fig. 5G) with only 1/9 showing a crystal agglomerate, the majority of cells transfected with the R704X *clc-5* mutant construct had associated crystal agglomerates (7/10, $p < 0.05$). Thus, in this separate experimental paradigm, annexin A2 located at the cell periphery was associated with increased crystal retention and agglomeration.

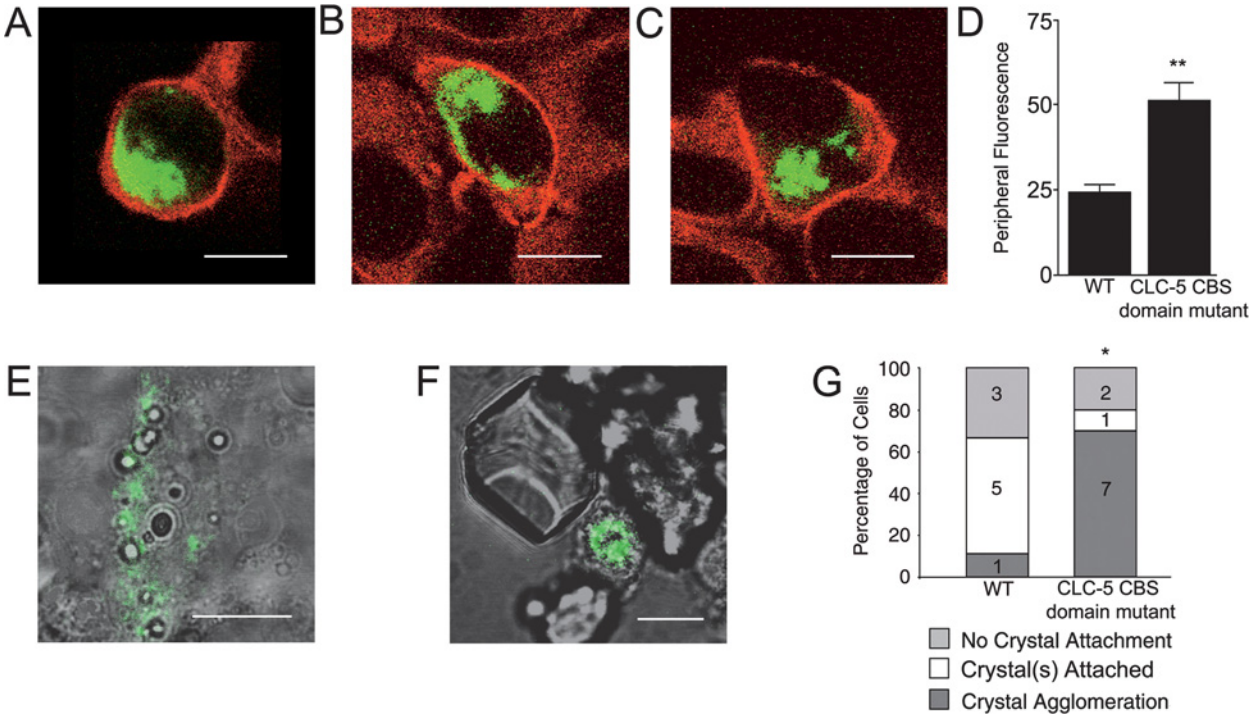

Figure 5. *clc-5* mutant transfection leads to redistribution of annexin A2 and crystal agglomeration in mIMCD-3 cells. Scale bar, 10 µm. Transfection with mutant *clc-5* constructs R648X (*A*), 695delCfs (*B*) and R704X (*C*) all cause a redistribution of annexin A2 towards the cell periphery, compared to surrounding non-transfected cells (and to *clc-5-GFP*-transfected cells; see fig. 2A). (*D*) Quantification of annexin A2 immunofluorescence at the cell periphery in mutant *clc-5* transfectants was (arbitrary units) 51.14 ± 5.34, n = 13 compared to 24.22 ± 2.13, n = 8, (**$p < 0.005$) in wild-type *clc-5-GFP*-transfected (WT) cells. (*E–G*) Comparison of mIMCD-3 cells transiently transfected with *clc-5-GFP* (*E*) or *GFP*-tagged mutant *clc-5* (R704X truncation) (*F*) when overlaid with preformed COM crystals. (*G*) Quantification of crystal attachment: WT transfectants displayed attached crystals (≤10 µm length) (5/9 cells) or no crystal attachment (3/9 cells) and rarely showed adhesion of crystal agglomerates (1/9 cells). In contrast, 7/10 mutant *clc-5* transfectants showed adhesion of crystal agglomerates (>10 µm) (*$p < 0.05$).

Membrane sialic acid residues also play a role in COM crystal agglomeration. Together with annexin A2, a number of membrane surface residues including specific sialic acid-containing glycoproteins, and possibly glycolipids (sialoglycoconjugates), are determinants of nucleation of calcium oxalate crystals on the apical surface of renal cells [39, 40]. The involvement of sialic acid residues was tested using mIMCD-3 cells, 24 h post-transfection with control *GFP*, sense *clc-5* and *GFP* or antisense *clc-5* and *GFP*, after preincubation with WGA lectin prior to crystal exposure. First, with no WGA lectin preincubation, control *GFP*-transfected cells and sense *clc-5*/*GFP* cotransfected cells behaved similarly (fig. 6A), with either an absence of crystals (9/11 and 9/13 cells, respectively) or small sized-crystal (≤10 µm length) attachments (2/11 and 4/13 cells, respectively). However, antisense *clc-5* transfection promoted pronounced crystal adherence leading to agglomeration (fig. 6A) similar to that shown in figure 3E.

For control and sense *clc-5* transfectants, WGA lectin pretreatment before calcium oxalate crystal exposure did not substantially alter the pattern of crystal retention; the majority of control *GFP* and sense *clc-5*/*GFP* cotransfected cells showed no crystal attachment (14/14 and 6/8 cells, respectively; fig. 6B). Importantly, there was a dramatic change in the pattern of crystal attachment to antisense transfected cells; WGA lectin caused a reduction in the number of cells with agglomerations from 87% to 20% ($p < 0.005$). This effect was lectin specific. Preincubation of transfectants with TRITC-concanavalin A (100 µg/ml, 2 min, 37 °C) had no effect on the marked crystal retention and agglomeration observed in antisense *clc-5* transfectants (15/21 cells possessing agglomerates) compared to sense *clc-5* or *GFP* transfectants (0/10 and 1/5 cells possessing agglomerates, respectively, $p < 0.005$).

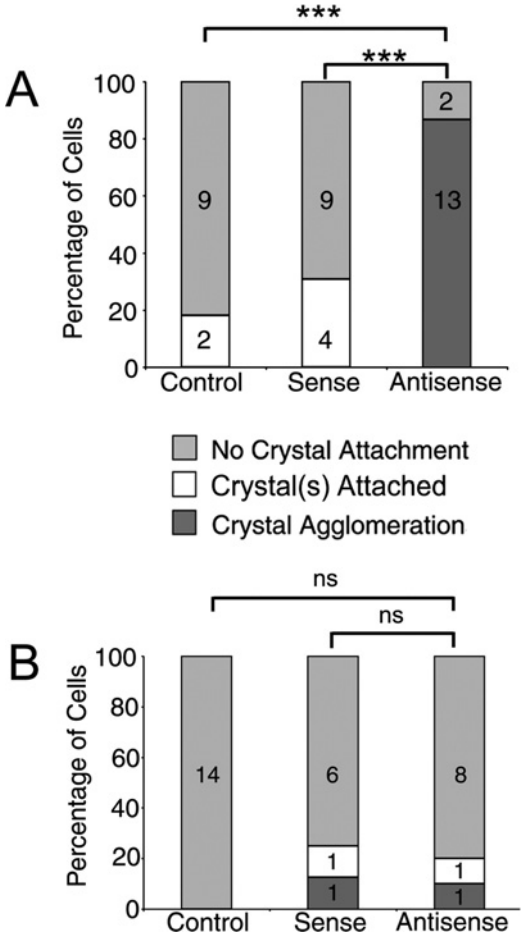

Figure 6. Antisense *clc-5* transfection promotes calcium oxalate crystal agglomeration that is blocked by pre-exposure to WGA lectin. Quantification of crystal attachment to transfected cells. (*A*) Pretreatment with media (2 min, 37 °C) before calcium oxalate crystal exposure: control (*GFP* alone) or sense *clc-5* and *GFP* showed either no crystal attachment (9/11 and 9/13, respectively) or small sized-crystal (10 µm length) attachments (2/11 and 4/13, respectively). Antisense *clc-5* transfectants (with *GFP* marker) demonstrated marked crystal agglomeration (13/15, ***$p < 0.005$) compared to both control and sense transfectants. (*B*) Pretreatment with TRITC-WGA lectin (100 µg/ml, 2 min, 37 °C). In the majority of control, sense or antisense transfected cells pretreated with WGA lectin, there was no crystal attachment (14/14, 6/8, 8/10, respectively).

Discussion

Nephrocalcinosis and nephrolithiasis are the end result of complex processes involving the composition of the tubular fluid favouring crystal formation followed by crystal retention and accumulation within the kidney. Crystal retention depends upon the ability of crystals to adhere to the renal tubular epithelial cell surface despite the presence of intrinsic mechanisms that minimize crystal formation, binding and retention. Recent atomic force microscopy (AFM) data using a negatively charged carboxyl AFM tip probe to measure adhesive force on individual COM crystal faces [41] shows that tip interaction to intercalate with Ca^{2+} at the crystal surface is highly specific and sensitive to the presence of protein components and solution anions. Such specificity in the ability of COM crystals to bind different cell surfaces is well documented. For example, calcium oxalate crystals do not adhere to the transitional epithelium of the bladder [42] but bind avidly to the surface of cells not normally exposed to crystals such as red blood cells [43] and endothelial cells [44]. A similar pattern is observed within the nephron. Verkoelen et al. [45] compared cell lines representative of the renal proximal tubule (LLC-PK1) with those of the distal/collecting duct (MDCK). Crystal binding was observed with the proximal tubule cells and, unlike the collecting duct cells, did not decrease as the cells reached confluency, indicating that epithelial cells along the nephron possess specific crystal-binding molecules at their luminal surface. Specific urinary anions such as py-

rophosphate and citrate, and negatively charged macromolecules, e.g. glycosaminoglycans, uropontin and nephrocalcin, can bind/coat crystals inhibiting crystal attachment to the cell surface. Once bound, crystals may also be removed from the apical surface by a process of endocytic uptake to a cellular location [46].

The present work sought to test the hypothesis that disruption of endogenous clc-5 (to mimic Dent's disease) in a collecting duct cell model system (mIMCD-3) results in alteration of the surface binding properties of a putative crystal binding molecule, annexin A2. This may explain the crystal binding and agglomeration for both calcium oxalate (COM) and calcium phosphate crystals previously demonstrated when mIMCD-3 cells were transfected with antisense *clc-5* constructs. Our previous work established that in these conditions, *clc-5* protein is markedly reduced, resulting in a reduction in the number of recycling acidic endosomes and an arrest of endocytosis [14, 15]. It is known in mouse proximal tubule cells from *clc-5* knockout mice that there is a reduction in the amount of the apical brush-border multiligand receptors, megalin and cubulin, from the apical membrane [9], together with the apical transporter proteins, Na-Pi2 and NHE3 [8]. This is most likely to arise from a redistribution of protein between the membrane and recycling vesicles, recycling being slowed (by luminal parathyroid hormone) [8].

Annexin A2 is expressed in renal epithelial cell lines including MDCK cells [47, 48] and has been shown to be expressed in the rat inner medullary collecting duct, with expression increasing following vasopressin treatment [49]. Similarly, annexin A2 is expressed in mIMCD-3 cells. Using transient transfection of *annexin* A2-*GFP*, we demonstrated that *annexin A2-GFP* is associated with several intracellular organelle markers, including those for the ER, Golgi apparatus and a subset of acidic endosomes. Consistent with a cytosolic and vesicular localization, annexin A2 has been localized to raft-associated sucrase-isomaltase-carrying vesicles in MDCK cells [50]. In addition, annexin A2 has previously been localized to endosomes in baby hamster kidney (BHK), rat basophilic leukemia cells [51, 52] and in Chinese hamster ovary (CHO) cells [53]. Our data confirm that the extensive cytosolic distribution of annexin A2 includes a subset of acidic endosomes. There is also colocalization of a minor fraction of annexin A2 at the plasma membrane of normal mIMCD-3 cells.

We were able to clearly demonstrate a redistribution of cellular annexin A2 to the cell periphery following antisense *clc-5* transfection or overexpression of mutant *clc-5* cDNAs. Members of the annexin family are characterized by the ability to bind phospholipids in a calcium-dependent manner, and a conserved structural element, the so-called annexin repeat [22], located in the carboxy-terminus which harbours the calcium- and membrane-binding sites. In the amino-terminus, there is a specific binding site for the small dimeric S100 protein, S100A10, with protein-protein interaction leading to the formation of a heterotetrameric complex. In this complex, two annexin A2 molecules are non-covalently linked via an S100A10 dimer bound to their NH_2-terminal domains [54]. This structure is compatible with a role in membrane vesicles and docking for binding from the cytoplasmic face. As already noted, proximal tubule cells in *clc-5* knockout mice show a reduced apical membrane expression of megalin, cubulin, NaPi-2 and NHE3 [8, 9]. If annexin A2 is involved in vesicular traffic between the cytosol and the plasma membrane, how is it possible to explain increased membrane annexin A2? Importantly, a further trafficking defect in proximal tubule cells of clc-5 knockout mouse kidneys involves impaired progression towards lysosomes [9]. Impaired vacuolar acidification (by ablation of *clc-5*) is known to prevent progression towards lysosomes, thereby rerouting endocytic tracers and newly synthesized lysosomal enzymes to the recycling pathway [9]. Disruption of clc-5 leading to an arrest of endocytosis in transfected cells combined with rerouting to the recycling pathway would be compatible with increased plasma membrane annexin A2 observed in the present experiments.

Kumar et al. [16] reported that annexin A2 is present on the exofacial surface of renal epithelial cell membranes [16]. Importantly, they noted that blocking surface annexin A2 with anti-annexin A2 antibody reduced COM crystal binding. Our own data show that anti-annexin A2 antibody preincubation reduces calcium oxalate crystal adhesion and agglomeration seen by endogenous clc-5 disruption. Given the N-terminal epitope of this antibody, the most likely explanation is that a fraction of the peripheral annexin A2 must be present on the exofacial part of the plasma membrane. This finding adds to the examples of cell surface annexin A2 functioning as a receptor for a number of polypeptide ligands including fetuin-A [55] or as a coreceptor for plasminogen in endothelial cells [56, 57].

Annexin A2 plasma membrane expression concurrent to crystal adhesion and agglomeration was also increased following mutant *clc-5* transfection. These truncated forms of *clc-5* omit the second CBS domain at the C-terminal tail and demonstrate pronounced trafficking defects [34]. A similar endocytic defect and a crystal agglomeration phenotype is observed with both truncated *clc-5* overexpression and antisense *clc-5* transfection. This suggests that these particular mutant *clc-5* constructs may have a dominant negative effect on endogenous clc-5 traffic via dimer formation.

Is annexin A2 the only crystal-binding molecule increased following antisense *clc-5* treatment? In the current study, calcium crystal agglomeration was also attenuated in antisense *clc-5* transfectants after blockade of

sialic acid residues by WGA lectin. The fact that a reduction in agglomeration towards control values was seen following treatment with anti-annexin A2 antibodies and by WGA lectin suggests that steric exclusion by bound protein at the cell surface contributes to inhibition of crystal binding. As already noted, other candidate adhesion molecules such as CD44, hyaluronan and osteopontin have been identified to function in both *in vitro* and *in vivo* models [35], showing that the complement of cell surface proteins in renal cells susceptible to crystal adhesion are likely to differ substantially from normal renal cells.

The clinical picture of Dent's disease patients invariably includes low molecular-weight proteinuria and hypercalciuria. How important is hypercalciuria to the subsequent development of nephrocalcinosis and nephrolithiasis? Nearly all of the affected males with Dent's disease have hypercalciuria [6, 58]. This correlates with almost 50% of Dent's disease patients having kidney stones [58] and two-thirds of patients displaying various degrees of medullary nephrocalcinosis [6, 58–60]. Thiazide diuretics, by reducing levels of urinary calcium excretion, seem to reduce stone disease [61] and renal failure and nephrocalcinosis were prevented by therapy with citrate, a crystal inhibitor, in the Johns Hopkins *clc-5* knockout mouse [62]. In the contrary situation, a murine model of Dent's disease without hypercalciuria failed to develop nephrocalcinosis [8, 63]. Thus we can infer that hypercalciuria promotes crystallization, which, in Dent's disease, seems to be intratubular in origin in both human [64] and animal studies [62]. It is known, however, that intratubular crystallization occurs in non-stone formers, but these crystals are smaller and less aggregated than in stone formers [13, 65, 66]. Therefore, the pathological events leading to renal stone disease and nephrocalcinosis in Dent's disease point to hypercalciuria and abnormal intratubular calcium crystal handling. The findings that adhesion molecules, such as annexin A2, are upregulated at the plasma membrane add weight to this argument.

In summary, Dent's disease causes both a reduction in acidification of endosomes and a failure of endocytosis [7, 8, 14, 63]. In the proximal tubule, this leads to altered plasma membrane protein expression, resulting in proteinuria, aminoaciduria, phosphaturia and hypercalciuria. More distally, where epithelial cells are exposed to calcium microcrystals, crystal adhesion surface molecules are also regulated by endocytic processes. We have shown that a disruption of clc-5 (mimicking Dent's disease) leads to an increase in annexin A2 expression at the plasma membrane of mIMCD-3 cells. Such an increase in plasma membrane annexin A2 results specifically in an enhanced calcium crystal-binding capacity, leading to crystal agglomeration. We hypothesize that disordered endocytosis within collecting duct cells leads to abnormal expression of crystal adhesion molecules contributing to the nephrocalcinosis and nephrolithiasis seen in affected patients with Dent's disease.

Acknowledgements. We thank Kidney Research UK for generous support.

1 Picollo A. and Pusch M. (2005) Chloride/proton antiporter activity of mammalian CLC proteins ClC-4 and ClC-5. Nature **436:** 420–423
2 Scheel O., Zdebik A. A., Lourdel S. and Jentsch T. J. (2005) Voltage-dependent electrogenic chloride/proton exchange by endosomal CLC proteins. Nature **436:** 424–427
3 Lloyd S. E., Pearce S. H., Fisher S. E., Steinmeyer K., Schwappach B., Scheinman S. J. et al. (1996) A common molecular basis for three inherited kidney stone diseases. Nature **379:** 445–449
4 Devuyst O., Christie P. T., Courtoy P. J., Beauwens R. and Thakker R. V. (1999) Intra-renal and subcellular distribution of the human chloride channel, CLC-5, reveals a pathophysiological basis for Dent's disease. Hum. Mol. Genet. **8:** 247–257
5 Obermuller N., Gretz N., Kriz W., Reilly R. F. and Witzgall R. (1998) The swelling-activated chloride channel ClC-2, the chloride channel ClC-3, and ClC-5, a chloride channel mutated in kidney stone disease, are expressed in distinct subpopulations of renal epithelial cells. J. Clin. Invest. **101:** 635–642
6 Wrong O. M., Norden A. G. and Feest T. G. (1994) Dent's disease: a familial proximal renal tubular syndrome with low-molecular-weight proteinuria, hypercalciuria, nephrocalcinosis, metabolic bone disease, progressive renal failure and a marked male predominance. QJM **87:** 473–493
7 Gunther W., Luchow A., Cluzeaud F., Vandewalle A. and Jentsch T. J. (1998) ClC-5, the chloride channel mutated in Dent's disease, colocalizes with the proton pump in endocytotically active kidney cells. Proc. Natl. Acad. Sci. USA **95:** 8075–8080
8 Piwon N., Gunther W., Schwake M., Bosl M. R. and Jentsch T. J. (2000) ClC-5 Cl^--channel disruption impairs endocytosis in a mouse model for Dent's disease. Nature **408:** 369–373
9 Christensen E. I., Devuyst O., Dom G., Nielsen R., Van der Smissen P., Verroust P. et al. (2003) Loss of chloride channel ClC-5 impairs endocytosis by defective trafficking of megalin and cubilin in kidney proximal tubules. Proc. Natl. Acad. Sci. USA **100:** 8472–8477
10 Wang S. S., Devuyst O., Courtoy P. J., Wang X. T., Wang H., Wang Y. et al. (2000) Mice lacking renal chloride channel, CLC-5, are a model for Dent's disease, a nephrolithiasis disorder associated with defective receptor-mediated endocytosis. Hum. Mol. Genet. **9:** 2937–2945
11 Luyckx V. A., Leclercq B., Dowland L. K. and Yu A. S. (1999) Diet-dependent hypercalciuria in transgenic mice with reduced CLC5 chloride channel expression. Proc. Natl. Acad. Sci. USA **96:** 12174–12179
12 Lieske J. C., Norris R. and Toback F. G. (1997) Adhesion of hydroxyapatite crystals to anionic sites on the surface of renal epithelial cells. Am. J. Physiol. **273:** F224–F233
13 Sayer J. A., Carr G. and Simmons N. L. (2004) Nephrocalcinosis: molecular insights into calcium precipitation within the kidney. Clin. Sci. (Lond.) **106:** 549–561
14 Sayer J. A., Carr G., Pearce S. H., Goodship T. H. and Simmons N. L. (2003) Disordered calcium crystal handling in antisense CLC-5-treated collecting duct cells. Biochem. Biophys. Res. Commun. **300:** 305–310
15 Sayer J. A., Carr G. and Simmons N. L. (2004) Calcium phosphate and calcium oxalate crystal handling is dependent upon CLC-5 expression in mouse collecting duct cells. Biochim. Biophys. Acta. **1689:** 83–90

16 Kumar V., Farell G., Deganello S. and Lieske J. C. (2003) Annexin II is present on renal epithelial cells and binds calcium oxalate monohydrate crystals. J. Am. Soc. Nephrol. **14:** 289–297
17 Montaville P., Neumann J. M., Russo-Marie F., Ochsenbein F. and Sanson A. (2002) A new consensus sequence for phosphatidylserine recognition by annexins. J. Biol. Chem. **277:** 24684–24693
18 Waisman D. M. (1995) Annexin II tetramer: structure and function. Mol. Cell. Biochem. 149–1**50:** 301–322
19 Donnelly S. R. and Moss S. E. (1997) Annexins in the secretory pathway. Cell. Mol. Life Sci. **53:** 533–538
20 Gerke V. and Moss S. E. (1997) Annexins and membrane dynamics. Biochim. Biophys Acta. **1357:** 129–154
21 Moss S. E. (1995) Ion channels: annexins taken to task. Nature **378:** 446–447
22 Gerke V. and Moss S. E. (2002) Annexins: from structure to function. Physiol. Rev. **82:** 331–371
23 Zobiack N., Rescher U., Ludwig C., Zeuschner D. and Gerke V. (2003) The annexin 2/S100A10 complex controls the distribution of transferrin receptor-containing recycling endosomes. Mol. Biol. Cell. **14:** 4896–4908
24 Creutz C. E., Moss S., Edwardson J. M., Hide I. and Gomperts B. (1992) Differential recognition of secretory vesicles by annexins. Biochem. Biophys. Res. Commun. **184:** 347–352
25 Emans N., Gorvel J. P., Walter C., Gerke V., Kellner R., Griffiths G. et al. (1993) Annexin II is a major component of fusogenic endosomal vesicles. J. Cell Biol. **120:** 1357–1369
26 Harder T. and Gerke V. (1993) The subcellular distribution of early endosomes is affected by the annexin II2p11(2) complex. J. Cell Biol. **123:** 1119–1132
27 Eberhard D. A. and Vandenberg S. R. (1998) Annexins I and II bind to lipid A: a possible role in the inhibition of endotoxins. Biochem. J. **330:** 67–72
28 Raynor C. M., Wright J. F., Waisman D. M. and Pryzdial E. L. (1999) Annexin II enhances cytomegalovirus binding and fusion to phospholipid membranes. Biochemistry **38:** 5089–5095
29 Baran D. T., Quail J. M., Ray R. and Honeyman T. (2000) Binding of 1alpha, 25-dihydroxyvitamin D(3) to annexin II: effect of vitamin D metabolites and calcium. J. Cell Biochem. **80:** 259–265
30 Ma K., Simantov R., Zhang J. C., Silverstein R., Hajjar K. A. and McCrae K. R. (2000) High affinity binding of beta 2-glycoprotein I to human endothelial cells is mediated by annexin II. J. Biol. Chem. **275:** 15541–15548
31 Hajjar K. A., Jacovina A. T. and Chacko J. (1994) An endothelial cell receptor for plasminogen/tissue plasminogen activator. I. Identity with annexin II. J. Biol. Chem. **269:** 21191–21197
32 Chung C. Y. and Erickson H. P. (1994) Cell surface annexin II is a high affinity receptor for the alternatively spliced segment of tenascin-C. J. Cell Biol. **126:** 539–548
33 Lieske J. C., Leonard R., Swift H. and Toback F. G. (1996) Adhesion of calcium oxalate monohydrate crystals to anionic sites on the surface of renal epithelial cells. Am. J. Physiol. **270:** F192–F199
34 Verhulst A., Asselman M., Persy V. P., Schepers M. S., Helbert M. F., Verkoelen C. F. et al. (2003) Crystal retention capacity of cells in the human nephron: involvement of CD44 and its ligands hyaluronic acid and osteopontin in the transition of a crystal-binding into a nonadherent epithelium. J. Am. Soc. Nephrol. **14:** 107–115
35 Asselman M., Verhulst A., De Broe M. E. and Verkoelen C. F. (2003) Calcium oxalate crystal adherence to hyaluronan-, osteopontin-, and CD44-expressing injured/regenerating tubular epithelial cells in rat kidneys. J. Am. Soc. Nephrol. **14:** 3155–3166
36 Sayer J. A., Stewart G. S., Boese S. H., Gray M. A., Pearce S. H. S., Goodship T. H. J. et al. (2001) The voltage-dependent Cl^- channel ClC-5 and plasma membrane Cl^- conductances of mouse renal collecting duct cells (mIMCD-3). J. Physiol. (Lond.) **536:** 769–783
37 Carr G., Simmons N. and Sayer J. (2003) A role for CBS domain 2 in trafficking of chloride channel CLC-5. Biochem. Biophys. Res. Commun. **310:** 600–605
38 Dutzler R., Campbell E. B., Cadene M., Chait B. T. and MacKinnon R. (2002) X-ray structure of a ClC chloride channel at 3.0 A reveals the molecular basis of anion selectivity. Nature **415:** 287–294
39 Lieske J. C., Toback F. G. and Deganello S. (2001) Sialic acid-containing glycoproteins on renal cells determine nucleation of calcium oxalate dihydrate crystals. Kidney Int. **60:** 1784–1791
40 Farell G., Huang E., Kim S. Y., Horstkorte R. and Lieske J. C. (2004) Modulation of proliferating renal epithelial cell affinity for calcium oxalate monohydrate crystals. J. Am. Soc. Nephrol. **15:** 3052–3062
41 Sheng X., Jung T., Wesson J. A. and Ward M. D. (2005) Adhesion at calcium oxalate crystal surfaces and the effect of urinary constituents. Proc. Natl. Acad. Sci. USA **102:** 267–272
42 Gill W. B., Jones K. W. and Ruggiero K. J. (1982) Protective effects of heparin and other sulfated glycosaminoglycans on crystal adhesion to injured urothelium. J. Urol. **127:** 152–154
43 Elferink J. G. (1987) The mechanism of calcium oxalate crystal-induced haemolysis of human erythrocytes. Br. J. Exp. Pathol. **68:** 551–557
44 Falasca G. F., Ramachandrula A., Kelley K. A., O'Connor C. R. and Reginato A. J. (1993) Superoxide anion production and phagocytosis of crystals by cultured endothelial cells. Arthritis Rheum. **36:** 105–116
45 Verkoelen C. F., Boom B. G. van der, Kok D. J., Houtsmuller A. B., Visser P., Schroder F. H. et al. (1999) Cell type-specific acquired protection from crystal adherence by renal tubule cells in culture. Kidney Int. **55:** 1426–1433
46 Lieske J. C. and Toback F. G. (1993) Regulation of renal epithelial cell endocytosis of calcium oxalate monohydrate crystals. Am. J. Physiol. **264:** F800–F807
47 Lee D. B. N., Jamgotchian N., Allen S. G., Kan F. W. K. and Hale I. L. (2004) Annexin A2 heterotetramer: role in tight junction assembly. Am. J. Physiol. **287:** F481–F491
48 Benaud C., Gentil B. J., Assard N., Court M., Garin J., Delphin C. et al. (2004) AHNAK interaction with the annexin 2/S100A10 complex regulates cell membrane cytoarchitecture. J. Cell Biol. **164:** 133–144
49 Balkom B. W. van, Hoffert J. D., Chou C. L. and Knepper M. A. (2004) Proteomic analysis of long-term vasopressin action in the inner medullary collecting duct of the Brattleboro rat. Am. J. Physiol. **286:** F216–F224
50 Jacob R., Heine M., Eikemeyer J., Frerker N., Zimmer K. P., Rescher U. et al. (2004) Annexin II is required for apical transport in polarized epithelial cells. J. Biol. Chem. **279:** 3680–3684
51 Merrifield C. J., Rescher U., Almers W., Proust J., Gerke V., Sechi A. S. et al. (2001) Annexin 2 has an essential role in actin-based macropinocytic rocketing. Curr. Biol. **11:** 1136–1141
52 Jost M., Zeuschner D., Seemann J., Weber K. and Gerke V. (1997) Identification and characterization of a novel type of annexin-membrane interaction: Ca^{2+} is not required for the association of annexin II with early endosomes. J. Cell Sci. **110:** 221–228
53 Trischler M., Stoorvogel W. and Ullrich O. (1999) Biochemical analysis of distinct Rab5- and Rab11-positive endosomes along the transferrin pathway. J. Cell Sci. **112:** 4773–4783
54 Lewit-Bentley A., Rety S., Sopkova-de Oliveira Santos J. and Gerke V. (2000) S100-annexin complexes: some insights from structural studies. Cell. Biol. Int. **24:** 799–802
55 Kundranda M. N., Ray S., Saria M., Friedman D., Matrisian L. M., Lukyanov P. et al. (2004) Annexins expressed on the cell

surface serve as receptors for adhesion to immobilized fetuin-A. Biochim. Biophys. Acta. **1693:** 111–123
56 Ling Q., Jacovina A. T., Deora A., Febbraio M., Simantov R., Silverstein R. L. et al. (2004) Annexin II regulates fibrin homeostasis and neoangiogenesis *in vivo*. J. Clin. Invest. **113:** 38–48
57 Kim J. and Hajjar K. A. (2002) Annexin II: a plasminogen-plasminogen activator co-receptor. Front. Biosci. **7:** d341–d348
58 Reinhart S. C., Norden A. G., Lapsley M., Thakker R. V., Pang J., Moses A. M. et al. (1995) Characterization of carrier females and affected males with X-linked recessive nephrolithiasis. J. Am. Soc. Nephrol. **5:** 1451–1461
59 Frymoyer P. A., Scheinman S. J., Dunham P. B., Jones D. B., Hueber P. and Schroeder E. T. (1991) X-linked recessive nephrolithiasis with renal failure. N. Engl. J. Med. **325:** 681–686
60 Hoopes R. R. Jr, Hueber P. A., Reid R. J. Jr, Braden G. L., Goodyer P. R., Melnyk A. R. et al. (1998) CLCN5 chloride-channel mutations in six new North American families with X-linked nephrolithiasis. Kidney Int. **54:** 698–705
61 Raja K. A., Schurman S., D'Mello R, G., Blowey D., Goodyer P., Van Why S. et al. (2002) Responsiveness of hypercalciuria to thiazide in Dent's disease. J. Am. Soc. Nephrol. **13:** 2938–2944
62 Cebotaru V., Kaul S., Devuyst O., Cai H., Racusen L., Guggino W. B. et al. (2005) High citrate diet delays progression of renal insufficiency in the ClC-5 knockout mouse model of Dent's disease. Kidney Int. **68:** 642–652
63 Gunther W., Piwon N. and Jentsch T. J. (2003) The ClC-5 chloride channel knock-out mouse – an animal model for Dent's disease. Pflugers Arch. **445:** 456–462
64 Moulin P., Igarashi T., Van der Smissen P., Cosyns J. P., Verroust P., Thakker R. V. et al. (2003) Altered polarity and expression of H^+-ATPase without ultrastructural changes in kidneys of Dent's disease patients. Kidney Int. **63:** 1285–1295
65 Herrmann U., Schwille P. O. and Kuch P. (1991) Crystalluria determined by polarization microscopy: technique and results in healthy control subjects and patients with idiopathic recurrent calcium urolithiasis classified in accordance with calciuria. Urol. Res. **19:** 151–158
66 Robertson W. G. and Peacock M. (1972) Calcium oxalate crystalluria and inhibitors of crystallization in recurrent renal stone-formers. Clin. Sci. **43:** 499–506